

# Modeling the concentration dependence of diffusion in zeolites. II. Kinetic Monte Carlo simulations of benzene in Na-Y

Chandra Saravanan

*Department of Chemistry, University of Massachusetts, Amherst, MA 01003*

Scott M. Auerbach<sup>a)</sup>

*Departments of Chemistry and Chemical Engineering, University of Massachusetts, Amherst, Massachusetts 01003*

(Received 12 June 1997; accepted 14 August 1997)

We have performed kinetic Monte Carlo simulations of benzene diffusion in Na-Y at finite loadings for various temperatures to test the analytical theory presented in Paper I, immediately preceding this paper. Our theory and simulations assume that benzene molecules jump among  $S_{II}$  and W sites, located near  $Na^+$  ions in 6-rings and in 12-ring windows, respectively. The theory exploits the fact that supercages are identical on average, yielding  $D_{\theta} = \frac{1}{6}k_{\theta}a_{\theta}^2 = \kappa a_{\theta}^2/6\langle\tau_1\rangle[1 + K_{eq}(1 \rightarrow 2)]$ , where  $k_{\theta}$  is the cage-to-cage rate coefficient,  $K_{eq}(1 \rightarrow 2)$  is the  $W \rightarrow S_{II}$  equilibrium coefficient,  $\langle\tau_1\rangle$  is the mean W site residence time, and  $\kappa$  is the transmission coefficient for cage-to-cage motion. The simulations use fundamental rate coefficients calculated at infinite dilution for consistency with the theory in Paper I. Our theory for  $k_{\theta}$ ,  $K_{eq}(1 \rightarrow 2)$  and  $\langle\tau_1\rangle$  agrees quantitatively with simulation for various temperatures and loadings. The simulated transmission coefficient is nearly  $\frac{1}{2}$  for all but the highest loadings, qualitatively validating our mean field approximation. Comparison between our theory and experimental data shows excellent qualitative agreement with tracer zero-length column data, but also shows qualitative disagreement with both pulsed field gradient NMR and frequency response data. © 1997 American Institute of Physics. [S0021-9606(97)51543-1]

## I. INTRODUCTION

Significant effort has been devoted to understanding diffusion in zeolites,<sup>1,2</sup> since transport properties play a central role in catalytic and separation processes<sup>3</sup> using zeolites.<sup>4</sup> Understanding the diffusion of aromatics in faujasite type zeolites<sup>5-12</sup> is particularly important because of persistent discrepancies among different experimental probes of mobility.<sup>1</sup> We have recently reported the results of analysis and simulation that greatly simplify our picture of benzene diffusion in Na-Y at infinite dilution, by focusing on the dynamics of cage-to-cage motion.<sup>11,13-16</sup> At finite loadings, however, benzene diffusion is complicated by blocking of stable sites and by intracage benzene-benzene interactions that modify adsorption and activation energies. Despite these influences, measured diffusion coefficients for aromatics in Na-X and Na-Y exhibit a remarkably gentle concentration dependence for low to moderate loadings.<sup>1,17-21</sup> In the paper immediately preceding, denoted as Paper I, we derive simple analytical expressions for the temperature and loading dependence of benzene diffusion in Na-Y. In the present article we report the results of kinetic Monte Carlo (KMC) simulations<sup>11,22,23</sup> of benzene diffusion in Na-Y at finite loadings to test theoretical assumptions made in Paper I.

We make three basic approximations in Paper I that simplify benzene diffusion in Na-Y. In this system benzene has two predominant binding sites.<sup>8</sup> In the primary site, denoted as  $S_{II}$ , benzene is facially coordinated to a supercage 6-ring, 2.70 Å above Na(II). In the secondary site, denoted as W,

benzene is centered in the 12-ring window separating adjacent supercages. Our theory begins by assuming that instantaneous benzene occupancies in different Na-Y supercages are identical, a mean field approximation. We then assume that occupancies at  $S_{II}$  and W sites are either 0 or 1, a site blocking model, and that benzenes do not otherwise interact. Finally, we allow at most one W site occupant when some  $S_{II}$  sites are vacant, a leading order approximation, motivated by the greater stability of  $S_{II}$  sites.<sup>5,11,12</sup> Thus, the theory in Paper I entails a mean field-site blocking-leading order model for benzene diffusion in Na-Y. We can test the mean field and leading order approximations by performing KMC simulations of benzene in Na-Y with fundamental rate coefficients calculated at infinite dilution,<sup>11</sup> since these KMC simulations include fluctuations ignored by mean field theory and allow many W sites to be occupied. We will address the accuracy of the site blocking model in a forthcoming publication.<sup>24</sup> By comparing theory and simulation in this way, we can use theory to develop a better understanding of simulation results, and ultimately gain a deeper understanding of diffusion in zeolites. Below we will show that our analytical theory gives quantitative agreement with simulation, and qualitative agreement with experiment for low to moderate loadings.

The remainder of this paper is organized as follows: in Sec. II we describe the KMC methodology used to model benzene diffusion in Na-Y. In Sec. III we report the convergence properties of the simulation, in addition to the simulation lengths and times required for production runs. In Sec. IV we compare simulation and theory for various loadings and temperatures, finding quantitative agreement. Section V

<sup>a)</sup>Author to whom correspondence should be addressed.

compares theory and experiment, and in Sec. VI we give concluding remarks, speculating on extending our theory to include guest–guest interactions.

## II. SIMULATION METHODOLOGY

We perform kinetic Monte Carlo (KMC) simulations<sup>11,22,23</sup> in the canonical ensemble, i.e. keeping  $N$ ,  $V$  and  $T$  fixed. Although a simulation more closely modeling, e.g., a pulsed field gradient NMR experiment<sup>1,19</sup> would fix  $\mu$  rather than  $N$ , since sorption equilibrium involves fluctuations in  $N$ , time scales of creating and destroying particles in a grand canonical KMC simulation are not obvious. Fixing  $N$  is reasonable, though, since most zeolite particles are large enough to make the relative root mean square fluctuations in  $N$  rather small. In what follows the W and S<sub>II</sub> sites are denoted sites 1 and 2, respectively.

We apply the KMC algorithm to benzene diffusion in Na-Y by replacing the zeolite framework with a three-dimensional lattice of S<sub>II</sub> and W binding sites. Such a lattice model is known to accurately reproduce diffusive behavior when site residence times are much longer than travel times between sites.<sup>22,25</sup> For a given configuration of  $N$  random walkers, a process list consisting of hops from the set (S<sub>II</sub>→S<sub>II</sub>, S<sub>II</sub>→W, W→S<sub>II</sub> and W→W) is compiled for all molecules by determining target site vacancies. We have been careful to minimize redundancy in the algorithm that updates the process list, since relatively few processes are affected by single molecule jumps. A hop is made every KMC step and the system clock is updated with variable time steps.<sup>26</sup> For a given configuration,  $\gamma$ , the mean time elapsed before each hop is the inverse of the *total* rate coefficient, determined by summing over all rate coefficients in the process list.<sup>26</sup> Assuming that  $M$  jumps are allowed for all molecules in  $\gamma$ , the total rate coefficient within the site blocking model is given by:

$$\begin{aligned} \langle \Delta t(\gamma) \rangle^{-1} &= k_{\text{tot}}(\gamma) = \sum_{k=1}^{M(\gamma)} k_i & (2.1) \\ &= n_{1 \rightarrow 1}(\gamma) \cdot k_{1 \rightarrow 1} + n_{1 \rightarrow 2}(\gamma) \cdot k_{1 \rightarrow 2} \\ &\quad + n_{2 \rightarrow 1}(\gamma) \cdot k_{2 \rightarrow 1} + n_{2 \rightarrow 2}(\gamma) \cdot k_{2 \rightarrow 2}, & (2.2) \end{aligned}$$

where  $n_{i \rightarrow j}(\gamma)$  is the  $\gamma$ -dependent number of allowed jumps from site  $i = 1, 2$  to site  $j = 1, 2$ . The actual KMC time step for a given configuration is randomly chosen from a Poisson distribution so that  $\Delta t(\gamma) = -\ln(1-x_1)/k_{\text{tot}}(\gamma)$ , where  $x_1 \in [0, 1)$  is a uniform random deviate. The chosen time step is independent of the actual jump executed. To choose an actual jump we define process probabilities according to  $p_i \equiv \sum_{j=1}^i k_j / k_{\text{tot}}(\gamma)$  for  $i = 1, \dots, M(\gamma)$ . The  $j^{\text{th}}$  process is chosen when  $p_j \leq x_2 < p_{j+1}$ , where  $x_2 \in [0, 1)$  is another uniform random deviate. After making a jump, relevant ensemble averages are updated, the process list is updated, and a new time step and jump process are chosen at random.

In Paper I we exploit the fact that all supercages are identical on average, yielding  $D_\theta = \frac{1}{6} k_\theta a_\theta^2$  where  $a_\theta \approx 11 \text{ \AA}$  is the mean intercage jump length and  $1/k_\theta$  is the mean super-

cage residence time. Furthermore, we find that  $k_\theta = \kappa \cdot k_1 \cdot P_1$ , where  $P_1 = [1 + K_{\text{eq}}(1 \rightarrow 2)]^{-1}$  is the probability of occupying a W site,  $\langle \tau_1 \rangle = 1/k_1$  is the mean W site residence time, and  $\kappa$  is the transmission coefficient for cage-to-cage motion. In what follows we use KMC to calculate the concentration dependencies of  $K_{\text{eq}}(2 \rightarrow 1)$ ,  $\langle \tau_1 \rangle$ ,  $\kappa$  and  $k_\theta$  at  $T = 300 \text{ K}$  for one Na-Y unit cell, containing 32 S<sub>II</sub> sites and 16 W sites. In Paper I, we show that the essential physics of the site blocking model is captured with one Na-Y unit cell. A simulation containing  $N$  molecules gives  $N$  distinct values for each of these quantities. We require as a convergence criterion that all  $N$  values of  $K_{\text{eq}}(2 \rightarrow 1)$ ,  $\langle \tau_1 \rangle$ ,  $\kappa$  and  $k_\theta$  be numerically equivalent. Convergence of these quantities is discussed in the next section.

For each molecule,  $K_{\text{eq}}(2 \rightarrow 1) = T_1/T_2$  where  $T_1$  and  $T_2$  are the total simulation times spent at W and S<sub>II</sub> sites, respectively. In addition,  $\langle \tau_1 \rangle = T_1/N^\ddagger$  where  $N^\ddagger$  is the number of visits to W sites. Furthermore,  $\kappa = N_{\text{cc}}/N^\ddagger$  where  $N_{\text{cc}}$  is the number of cage-to-cage jumps for a given molecule. Finally,  $k_\theta = N_{\text{cc}}/(T_1 + T_2)$ . Note that  $\kappa$  and  $k_\theta$  require a definition of cage-to-cage jumping. Care must be taken in defining a cage-to-cage hop because W sites are shared by adjacent supercages. Although one solution to this difficulty is to assign W sites to particular supercages (two W sites per cage), we avoided this approach because the assignment is arbitrary and breaks Na-Y symmetry. Instead, we used the following approach: if for a given molecule the  $n^{\text{th}}$  KMC step is a W site, we calculate the distance between benzene center of mass positions for KMC steps  $n-1$  and  $n+1$ . If this distance is nonzero and different from the four characteristic intracage distances<sup>8</sup> [ $d(\text{S}_{\text{II}}, \text{S}_{\text{II}}) = 5.48 \text{ \AA}$ ,  $d(\text{S}_{\text{II}}, \text{W}) = 5.31 \text{ \AA}$ ,  $d(\text{S}_{\text{II}}, \text{W}') = 8.74 \text{ \AA}$ , and  $d(\text{W}, \text{W}) = 8.79 \text{ \AA}$ ], then a cage-to-cage jump is registered with  $t_{n+1}$  stored as the arrival time in the new cage. The residence time is the difference between  $t_{n+1}$  and the previously stored arrival time.

As part of the site blocking model, we use fundamental hopping rate coefficients calculated at infinite dilution to determine jump times and probabilities. In the present study, as in former ones,<sup>11,13–16,27</sup> we estimate rate coefficients at infinite dilution using the Arrhenius formula, in which  $k \equiv \nu e^{-\beta E_a}$  where  $\nu$  and  $E_a$  are temperature independent. We assume that the Arrhenius prefactors  $\{\nu\}$  resemble typical vibrational frequencies, of order  $10^{13} \text{ s}^{-1}$ . We believe these rate coefficients are sufficiently accurate for the purpose of drawing qualitative conclusions. The calculated hopping activation energies and hypothetical Arrhenius prefactors reported in Ref. 11 are summarized in Table I.

## III. SIMULATION CONVERGENCE

As mentioned above, convergence of a simulation containing  $N$  random walkers is obtained when all  $N$  molecules give numerically identical results. The equilibrium coefficient,  $K_{\text{eq}}(2 \rightarrow 1)$ , turns out to converge slowly for high loadings. Since we have exact expressions for this quantity from Paper I, we focus on its convergence properties. Also, since  $k_\theta$  is ultimately the quantity of interest, we study its

TABLE I. Hopping activation energies and hypothetical Arrhenius prefactors for benzene in Na-Y. Our model predicts that leaving the W site is relatively facile.

Jump	Activation energy (kJ mol <sup>-1</sup> )	Arrhenius prefactor (s <sup>-1</sup> )
S <sub>II</sub> →S <sub>II</sub>	35	10 <sup>13</sup>
S <sub>II</sub> →W	41	10 <sup>13</sup>
W→S <sub>II</sub>	16	10 <sup>13</sup>
W→W	18	10 <sup>13</sup>

convergence as well. The transmission coefficient converges extremely rapidly, and as such is not a focus of our convergence studies.

Figure 1 shows  $K_{\text{eq}}(2 \rightarrow 1)$  calculated with KMC divided by its exact value for  $N=20$  as a function of the number of KMC steps,  $N_{\text{KMC}}$ , for 8 molecules chosen at random. Figure 1 shows smooth convergence of  $K_{\text{eq}}(2 \rightarrow 1)$  to a relative error less than 2% at  $3 \times 10^6$  KMC steps. Figure 2 shows  $k_{\theta}$  calculated with KMC for  $N=20$  vs.  $N_{\text{KMC}}$  for 8 molecules chosen at random. Excellent convergence is obtained for  $k_{\theta}$  at  $N_{\text{KMC}}=3 \times 10^6$ , giving a relative spread less than 1%.

Figures 3 and 4 are the same as Figs. 1 and 2, except for  $N=40$ . Good convergence for both  $K_{\text{eq}}(2 \rightarrow 1)$  and  $k_{\theta}$  is obtained at high loading, although at much more computational expense. The relative error at  $100 \times 10^6$  KMC steps in Fig. 3 is less than 10%, while the spread at  $100 \times 10^6$  KMC steps in Fig. 4 is 7%.

Figure 5 compares exact and KMC results for  $K_{\text{eq}}(2 \rightarrow 1)$  at  $T=300$  K as a function of loading. The calculations in Fig. 5 use  $3 \times 10^6$  KMC steps for  $N \leq 32$  and  $100 \times 10^6$  KMC steps for  $N > 32$ . Excellent KMC convergence is obtained for all but the highest loadings, which give  $K_{\text{eq}}(2 \rightarrow 1)$  values that are consistently low by about 10%. As can be seen from Figs. 1–5,  $3 \times 10^6$  KMC steps suffice to

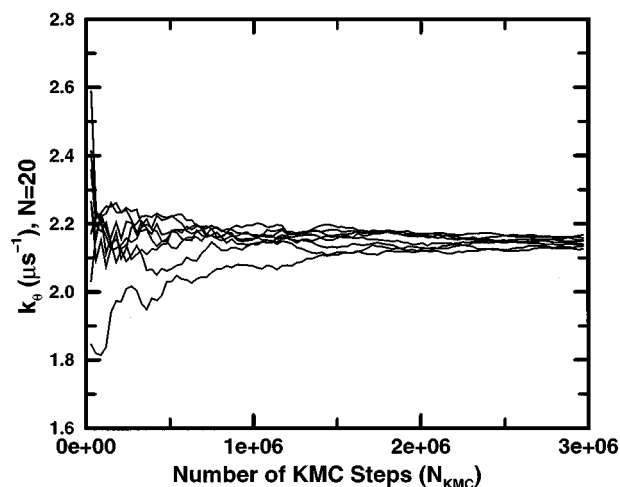


FIG. 2. KMC results for  $k_{\theta}$  for  $N=20$  vs.  $N_{\text{KMC}}$  for 8 molecules chosen at random. Spread at  $N_{\text{KMC}}=3 \times 10^6$  less than 1%.

give reasonably converged results for loadings  $N \leq 32$ , requiring 10 min of CPU time per loading on an IBM RS/6000 with a 604e 200 MHz processor. For loadings  $N > 32$ , reasonable convergence is obtained with  $100 \times 10^6$  KMC steps, requiring 7 hours of CPU time per loading on the same IBM RS/6000.

#### IV. COMPARISON BETWEEN THEORY AND SIMULATION

Figure 6 compares analytical theory and KMC results for  $\langle \tau_1 \rangle$  at  $T=300$  K as a function of loading. As discussed in Paper I, our theory for  $\langle \tau_1 \rangle$  is exact for  $N=1$  and 48, and should also be accurate near  $N=1$ , 32 and 48. Figure 6

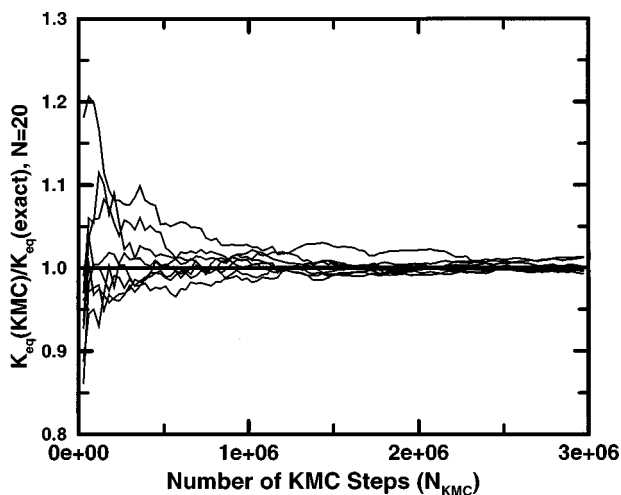


FIG. 1. Ratio of  $K_{\text{eq}}(2 \rightarrow 1)$  values from KMC and exact for  $N=20$  vs.  $N_{\text{KMC}}$  for 8 molecules chosen at random. Relative error at  $N_{\text{KMC}}=3 \times 10^6$  less than 2%.

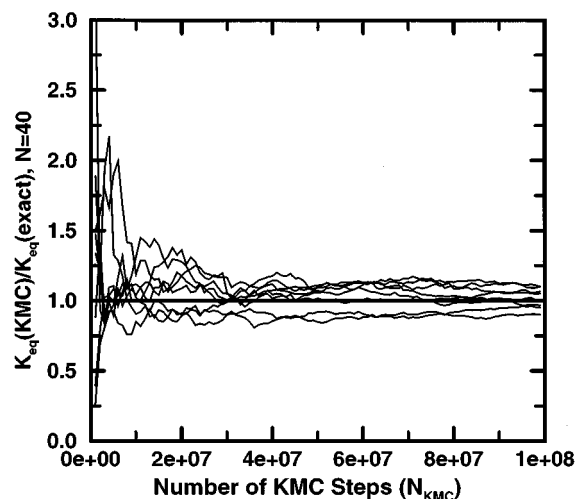


FIG. 3. Same as Fig. 1 except that  $N=40$ . Relative error at  $N_{\text{KMC}}=100 \times 10^6$  less than 10%.

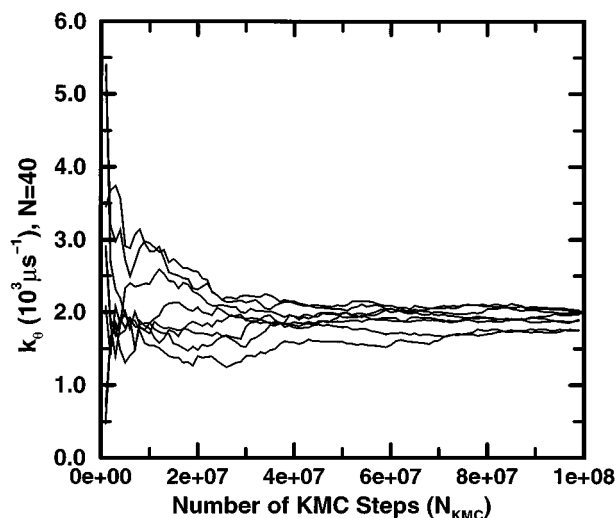


FIG. 4. Same as Fig. 2 except that  $N=40$ . Spread at  $N_{\text{KMC}}=100 \times 10^6$  is 7%.

shows the remarkable fact that our formulas for  $\langle \tau_1 \rangle$ , namely

$$\langle \tau_1 \rangle \cong \frac{1}{6k_{1 \rightarrow 1} + 6[1 - (N-1)/N_2]k_{1 \rightarrow 2}}, \quad \text{for } N \leq N_2 = 32 \quad (4.1)$$

$$\cong \frac{1}{6[1 - (N - N_2 - 1)/(N_1 - 1)]k_{1 \rightarrow 1}}, \quad \text{for } N > N_2 = 32, \quad (4.2)$$

exhibit quantitative agreement with KMC for *all* loadings. In complete agreement with simulation, Eqs. (4.1) and (4.2) show that the mean W site residence time increases monotonically with loading as target sites for  $W \rightarrow S_{\text{II}}$  and  $W \rightarrow W$  jumps become occupied. More generally, Fig. 6 shows that accurate results for a mean residence time in a fluctuating environment can be obtained by inverting the averaged rate coefficient [cf. Eq. (3.28) in Paper I], rather than averaging the inverted rate coefficient.

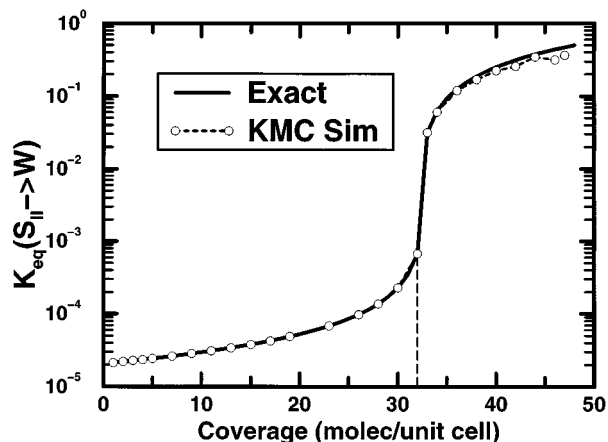


FIG. 5.  $K_{\text{eq}}(2 \rightarrow 1)$  at  $T=300$  K comparing exact and KMC results. Excellent convergence is obtained for most loadings.

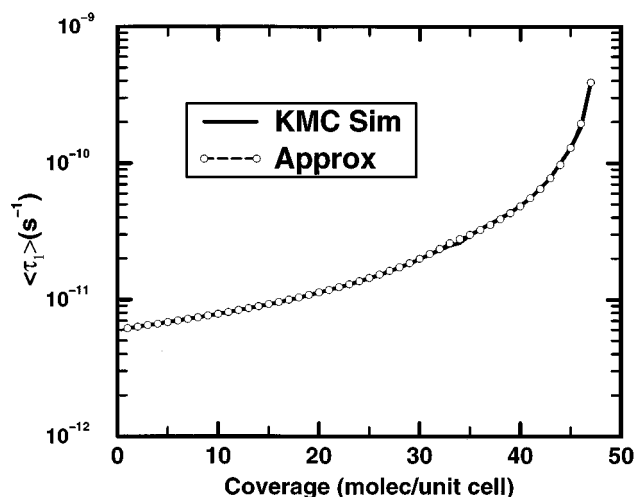


FIG. 6.  $\langle \tau_1 \rangle$  at  $T=300$  K comparing approximate analytical and KMC results. Excellent agreement with simulation is obtained for all loadings.

Figure 7 shows the comparison between our mean field approximation for the transmission coefficient, i.e.  $\kappa = \frac{1}{2}$  for all loadings, and the KMC results calculated at  $T=300$  K. The simulated transmission coefficient is less than or equal to  $\frac{1}{2}$  for all loadings, and for all but the highest loadings is within 10% of  $\frac{1}{2}$ . Figure 7 qualitatively validates our mean field approximation for low to moderate loadings. We will quantitatively address the accuracy of the mean field approximation in a forthcoming publication.<sup>28</sup> It is interesting to note that for  $N=33$ , with 1 molecule forced to occupy a W site, the system mimics infinite dilution since  $W \rightarrow W \rightarrow W$  jumps become the most probable mechanism of cage-to-cage motion.

Figure 8 shows the comparison between simulation and our overall analytical expression for the cage-to-cage rate coefficient at  $T=300$  K for one Na-Y unit cell. Excellent agreement between theory and simulation is obtained for

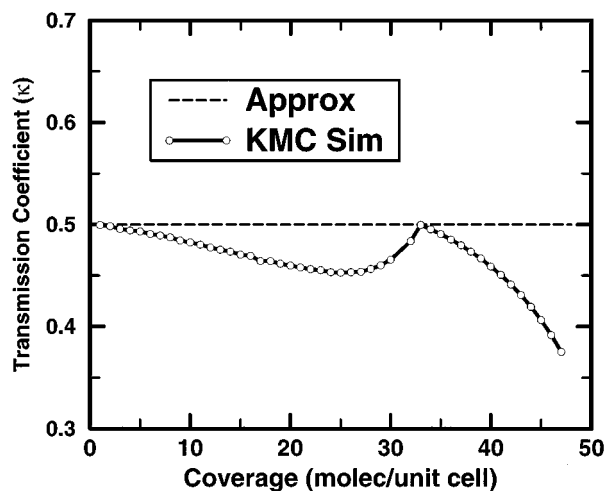


FIG. 7. Transmission coefficient,  $\kappa$ , at  $T=300$  K comparing approximate analytical and KMC results. Mean field approximation is qualitatively accurate for all but the highest loadings.

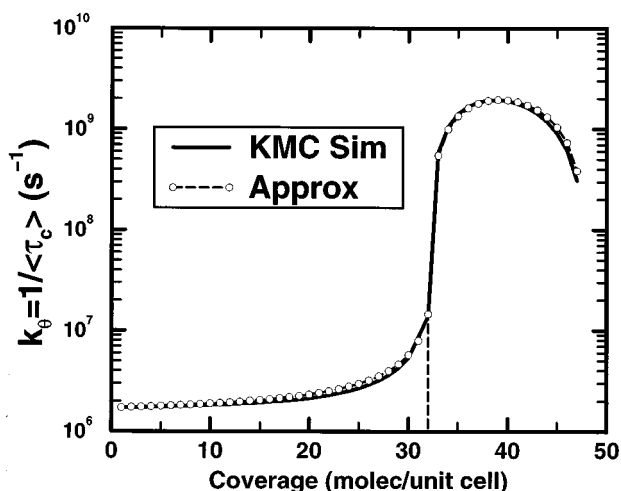


FIG. 8. Cage-to-cage rate coefficient,  $k_\theta$ , at  $T=300$  K comparing approximate analytical and KMC results. Excellent agreement between theory and simulation is obtained for all loadings. Error at high loading is from  $\kappa$ .

most loadings. The small error at the highest loadings derives from error in  $\kappa$ . The analytical formulas being tested in Fig. 8 are:

$$k_\theta \cong \frac{3}{2} \left( \frac{N_2}{N_2 - N + 1} \cdot \frac{k_{1 \rightarrow 1}}{k_{1 \rightarrow 2}} + 1 \right) k_{2 \rightarrow 1}, \quad \text{for } N \leq N_2 = 32 \quad (4.3)$$

$$\xrightarrow{v \rightarrow \infty} \frac{3}{2} \left( \frac{2}{2 - 3\theta} \cdot \frac{k_{1 \rightarrow 1}}{k_{1 \rightarrow 2}} + 1 \right) k_{2 \rightarrow 1}, \quad \text{for } \theta < \frac{2}{3} \quad (4.4)$$

$$\cong 3 \left( \frac{N_1 + N_2 - N}{N_1 - 1} \right) \left( \frac{N - N_2}{N} \right) k_{1 \rightarrow 1}, \quad \text{for } N > N_2 = 32 \quad (4.5)$$

$$\xrightarrow{v \rightarrow \infty} 3(1 - \theta) \left( \frac{3\theta - 2}{\theta} \right) k_{1 \rightarrow 1}, \quad \text{for } \theta > \frac{2}{3}. \quad (4.6)$$

Equations (4.3) and (4.5) reveal the essential physics displayed in Fig. 8. The simulated cage-to-cage rate coefficient increases at low loadings because of an entropic preference to occupy W sites as  $S_{II}$  sites become blocked. Diffusion within the site blocking model becomes precipitously faster above  $\theta = \frac{2}{3}$  as molecules are forced to occupy W sites, i.e. the operative temperature dependence changes from  $k_{2 \rightarrow 1}$  to  $k_{1 \rightarrow 1}$ . At the highest loadings, as almost all W sites become occupied, the W site residence time increases and slows diffusion.

According to Eq. (4.3),  $k_\theta$  for  $N \leq 32$  should exhibit an apparent activation energy approximately equal to  $E_a(2 \rightarrow 1) = 41 \text{ kJ mol}^{-1}$ , since  $E_a(1 \rightarrow 1) \cong E_a(1 \rightarrow 2)$  as given in Table I. Furthermore,  $k_\theta$  for  $N > 32$  should exhibit an apparent activation energy equal to  $E_a(1 \rightarrow 1) = 18 \text{ kJ mol}^{-1}$ . To test these predictions of our theory, we used KMC to calculate  $k_\theta$  for  $N=20$  and  $40$  at  $T=200$  K,  $300$  K and  $400$  K. These simulation results (thick lines) are compared with theory (open circles) in Fig. 9, which shows Arrhenius temperature dependencies for both loadings. The apparent activation energies for  $N=20$  are  $E_a$

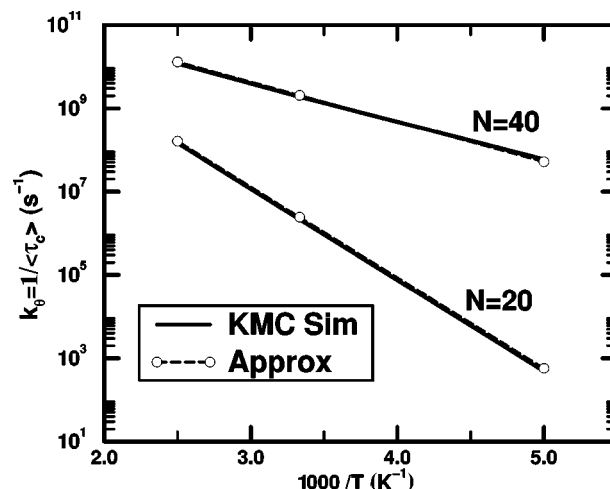


FIG. 9. Comparison between simulated and theoretical  $k_\theta$  for  $N=20$  and  $40$  at  $T=200$  K,  $300$  K, and  $400$  K. Very good agreement between theory and simulation is obtained, with small differences arising because  $\kappa < \frac{1}{2}$ .

$= 41.9 \text{ kJ mol}^{-1}$  from simulation and  $41.7 \text{ kJ mol}^{-1}$  from theory, in excellent agreement. Without an analytical expression for  $k_\theta$ , we might attribute the difference between the apparent activation energy from simulation and  $E_a(2 \rightarrow 1)$  to statistical error in the simulation. Equation (4.3) shows, however, that this difference arises from the additional temperature dependence in  $k_{1 \rightarrow 1}/k_{1 \rightarrow 2}$  associated with  $S_{II} \rightarrow W \rightarrow W$  cage-to-cage jumps. The Arrhenius prefactors for  $N=20$  are  $\nu = 4.3 \times 10^{13} \text{ s}^{-1}$  from simulation and  $4.5 \times 10^{13} \text{ s}^{-1}$  from theory, also in very good agreement. The small discrepancy in  $\nu$  arises because the simulated transmission coefficient,  $\kappa_{\text{sim}}$ , is slightly less than  $\frac{1}{2}$ .

For  $N=40$  excellent agreement between simulation and theory is also obtained for the temperature dependence of  $k_\theta$ . The apparent activation energies for  $N=40$  are  $E_a = 18.0 \text{ kJ mol}^{-1}$  from simulation and  $18 \text{ kJ mol}^{-1}$  from theory, as expected from Eq. (4.5) and Table I. The Arrhenius prefactors for  $N=40$  are  $\nu = 2.9 \times 10^{12} \text{ s}^{-1}$  from simulation and  $3.2 \times 10^{12} \text{ s}^{-1}$  from theory. This small difference in  $\nu$  also arises because  $\kappa_{\text{sim}} < \frac{1}{2}$ .

## V. COMPARISON BETWEEN THEORY AND EXPERIMENT

The strictest test of our theory is comparison with experiment. Unfortunately, experimental data on the concentration dependence of benzene self diffusion in Na-Y are rather sparse because Y-zeolite particles are relatively small, making reliable measurements of the mean square displacement difficult.<sup>29</sup> The most comparable data are diffusion coefficients for benzene in Na-X, measured by the tracer zero-length column (TZLC) method,<sup>21</sup> pulsed field gradient (PFG) NMR,<sup>19</sup> and the frequency response (FR) technique.<sup>20</sup> Comparing theory and experiment for different systems may lead to ambiguous results, since discrepancies can arise from approximations in the theory and from comparing different systems. Nonetheless, we feel that such comparisons, when

carefully made, are an important part of the evolving knowledge in the field.

Although all three experimental studies report self diffusion coefficients for benzene intracrystalline motion in Na-X, and thus should agree, they qualitatively disagree in magnitude and concentration dependence. For the loading  $\theta \cong 0.3$ , TZLC diffusivities are  $\sim 8$  times smaller than FR data and  $\sim 40$  times smaller than PFG NMR data. Furthermore, TZLC diffusivities increase with loading according to  $\log D_{\theta} \propto \theta$ , while both FR and PFG NMR diffusivities decrease with loading. As can be seen from Fig. 8, our site blocking theory predicts that  $k_{\theta}$  increases gently with loading according to  $\log k_{\theta} \propto \theta$  for low to moderate loadings, in excellent qualitative agreement with TZLC data. We need to incorporate guest-guest interactions more faithfully into our model before we can assert that the TZLC concentration dependence is actually correct. Nonetheless, it is interesting that this initial level of theory is quite consistent with the TZLC data.

## VI. CONCLUDING REMARKS

We have performed kinetic Monte Carlo (KMC) simulations of benzene diffusion in Na-Y at finite loadings for various temperatures to test the analytical diffusion theory presented in Paper I, immediately preceding this paper. The analytical diffusion theory exploits the fact that supercages are identical on average, yielding  $D_{\theta} = \frac{1}{6} k_{\theta} a_{\theta}^2$  where  $a_{\theta} \cong 11 \text{ \AA}$  and  $k_{\theta}$  is the cage-to-cage rate coefficient, given by  $\kappa \cdot k_1 \cdot P_1$ . Here  $P_1 = [1 + K_{\text{eq}}(1 \rightarrow 2)]^{-1}$  is the probability of occupying a W site,  $\langle \tau_1 \rangle = 1/k_1$  is the mean W site residence time, and  $\kappa$  is the transmission coefficient for cage-to-cage motion. In Paper I we obtain analytical expressions for these quantities by assuming that  $S_{\text{II}}$  and W site occupancies are either 0 or 1 and that benzenes do not otherwise interact. For consistency, the KMC simulations use fundamental hopping rate coefficients calculated at infinite dilution. The theoretical concentration dependencies of  $k_{\theta}$ ,  $K_{\text{eq}}(1 \rightarrow 2)$  and  $\langle \tau_1 \rangle$  give quantitative agreement with simulation for  $T = 200\text{--}400 \text{ K}$ . The simulated transmission coefficient is very close to the mean field value,  $\frac{1}{2}$ , for all but the highest loadings. We regard this as a qualitative validation of our mean field approximation. We will quantitatively address the accuracy of the mean field approximation in a forthcoming publication.<sup>28</sup> Thus, our analytical diffusion theory captures the essential physics of this site blocking model, allowing the site blocking KMC simulation results to be understood completely.

Comparison between site blocking theory and tracer zero-length column data shows excellent qualitative agreement, with  $\log D_{\theta} \propto \theta$  for low to moderate loadings. Comparing our theoretical results with pulsed field gradient NMR and with frequency response data yields qualitative disagreement. To add further validity to our model, we must include medium to long range guest-guest interactions. We will address the importance of these interactions in a forthcoming publication<sup>24</sup> by considering how nearest neighbor  $S_{\text{II}}$  and W site occupancies affect binding site stabilities and residence

times, in analogy with the Ising model of phase equilibrium.<sup>30</sup> Extending our KMC simulation methodology to include nearest neighbor interactions should be straightforward. We can also apply analytical mean field theory to the lattice model with nearest neighbor interactions to develop a theory of diffusion with site blocking and intracage interactions.

## ACKNOWLEDGMENTS

The authors thank Dr. Fabien Jousse and Professor Stefano Brandani for many stimulating discussions. S.M.A. acknowledges support from the NSF under grants CHE-9625735 and CHE-9616019, and from Molecular Simulations, Inc. for generously providing visualization software. Acknowledgment is made to the donors of the Petroleum Research Fund, administered by the American Chemical Society, for partial support of this research under grant ACS-PRF 30853-G5.

- <sup>1</sup>J. Kärger and D. M. Ruthven, *Diffusion in Zeolites and Other Microporous Solids* (Wiley, New York, 1992).
- <sup>2</sup>N. Y. Chen, T. F. Degnan, Jr., and C. M. Smith, *Molecular Transport and Reaction in Zeolites* (VCH, New York, 1994).
- <sup>3</sup>J. Weitkamp, in *Catalysis and Adsorption by Zeolites*, edited by G. Olmann, J. C. Vedrine, and P. A. Jacobs (Elsevier, Amsterdam, 1991).
- <sup>4</sup>J. M. Newsam, *Zeolites*, in *Solid State Chemistry: Compounds*, edited by A. K. Cheetham and P. Day (Oxford University Press, Oxford, 1992), pp. 234–280.
- <sup>5</sup>P. Demontis, S. Yashonath, and M. L. Klein, *J. Phys. Chem.* **93**, 5016 (1989).
- <sup>6</sup>L. M. Bull, N. J. Henson, A. K. Cheetham, J. M. Newsam, and S. J. Heyes, *J. Phys. Chem.* **97**, 11 776 (1993).
- <sup>7</sup>D. Barthomeuf and B. H. Ha, *J. Chem. Soc. Faraday Trans.* **69**, 2158 (1973).
- <sup>8</sup>A. N. Fitch, H. Jovic, and A. Renouprez, *J. Phys. Chem.* **90**, 1311 (1986).
- <sup>9</sup>L. Uytterhoeven, D. Dompas, and W. J. Mortier, *J. Chem. Soc. Faraday Trans.* **88**, 2753 (1992).
- <sup>10</sup>H. Klein, C. Kirschhock, and H. Fuess, *J. Phys. Chem.* **98**, 12345 (1994).
- <sup>11</sup>S. M. Auerbach, N. J. Henson, A. K. Cheetham, and H. I. Metiu, *J. Phys. Chem.* **99**, 10 600 (1995).
- <sup>12</sup>P. J. O'Malley and C. J. Braithwaite, *Zeolites* **15**, 198 (1995).
- <sup>13</sup>S. M. Auerbach and H. I. Metiu, *J. Chem. Phys.* **105**, 3753 (1996).
- <sup>14</sup>S. M. Auerbach, L. M. Bull, N. J. Henson, H. I. Metiu, and A. K. Cheetham, *J. Phys. Chem.* **100**, 5923 (1996).
- <sup>15</sup>S. M. Auerbach and H. I. Metiu, *J. Chem. Phys.* **106**, 2893 (1997).
- <sup>16</sup>S. M. Auerbach, *J. Chem. Phys.* **106**, 7810 (1997).
- <sup>17</sup>J. Kärger and D.M. Ruthven, *J. Chem. Soc. Faraday Trans. I* **77**, 1485 (1981).
- <sup>18</sup>M. Bülow, W. Mietk, P. Struve, and P. Lorenz, *J. Chem. Soc. Faraday Trans. I* **79**, 2457 (1983).
- <sup>19</sup>A. Germanus, J. Kärger, H. Pfeifer, N. N. Samulevic, and S. P. Zdanov, *Zeolites* **5**, 91 (1985).
- <sup>20</sup>D. M. Shen and L. V. C. Rees, *Zeolites* **11**, 666 (1991).
- <sup>21</sup>S. Brandani, Z. Xu, and D. Ruthven, *Microporous Mater.* **7**, 323 (1996).
- <sup>22</sup>R. L. June, A. T. Bell, and D. N. Theodorou, *J. Phys. Chem.* **95**, 8866 (1991).
- <sup>23</sup>K. A. Fichthorn and W. H. Weinberg, *J. Chem. Phys.* **95**, 1090 (1991).
- <sup>24</sup>C. Saravanan and S. M. Auerbach (in preparation).
- <sup>25</sup>R. Gomer, *Rep. Prog. Phys.* **53**, 917 (1990).
- <sup>26</sup>P. Maksym, *Semicond. Sci. Technol.* **3**, 594 (1988).
- <sup>27</sup>Chandra Saravanan and Scott M. Auerbach, *J. Chem. Phys.* **107**, 8120 (1997), preceding paper.
- <sup>28</sup>C. Saravanan and S. M. Auerbach (submitted).
- <sup>29</sup>J. Kärger (private communication).
- <sup>30</sup>D. Chandler, *Introduction to Modern Statistical Mechanics* (Oxford University Press, New York, 1987).